Progress in Biomaterials (2020) 9:25–34
https://doi.org/10.1007/s40204-020-00129-0

ORIGINAL RESEARCH

Enhanced biological properties of collagen/chitosan-coated poly(ε-caprolactone) scaffold by surface modification with GHK-Cu peptide and 58S bioglass

Amir Mahdi Molavi[1,2] · Alireza Sadeghi-Avalshahr[1,3] · Samira Nokhasteh[1] · Hojjat Naderi-Meshkin[4]

Received: 23 December 2019 / Accepted: 16 March 2020 / Published online: 4 April 2020

Abstract

Bioactive glasses and peptides have shown promising results in improving wound healing and skin repair. The present study explores the effectiveness of surface modification of collagen/chitosan-coated electrospun poly(ε-caprolactone) scaffold with 58S bioactive glass or GHK-Cu peptide. To coat scaffolds with the bioactive glass, we prepared suspensions of silanized bioactive glass powder with three different concentrations and the scaffolds were pipetted with suspensions. Similarly, GHK-Cu-coated scaffolds were prepared by pipetting adequate amount of 1-mM solution of peptide (in milli-Q) on the surface of scaffolds. ATR–FTIR spectroscopy indicated the successful modification of collagen/chitosan-coated electrospun poly(ε-caprolactone) scaffold with bioactive glass and GHK-Cu. Microstructural investigations and in vitro studies such as cell adhesion, cell viability and antibacterial assay were performed. All samples demonstrated desirable cell attachment. Compared to poly(ε-caprolactone)/collagen/chitosan, the cell proliferation of GHK-Cu and bioactive glass-coated (concentrations of 0.01 and 0.1) scaffolds increased significantly at days 3 and 7, respectively. Poly(ε-caprolactone)/collagen/chitosan-uncoated scaffold and scaffolds coated with GHK-Cu and bioactive glass revealed desirable antibacterial properties but the antibacterial activity of GHK-Cu-coated sample turned out to be superior. These findings indicated that biological properties of collagen/chitosan-coated synthetic polymer could be improved by GHK-Cu and bioactive glass.

Keywords GHK-cu · 58S bioactive glass · Biological properties · Skin tissue engineering

Introduction

To fulfill the essential demands for accelerating regeneration and relieving pain in the injured skin, many researches have focused on skin tissue engineering and great achievements have been made. For instance, both engineered autologous skin and synthetic skin substitutes are available in the market and natural biopolymers such as collagen, hyaluronic acid and glycosaminoglycan have improved biological properties of synthetic products (Vig et al. 2017; Boyce and Lalley 2018). Biodegradable synthetic polymers such as poly(lactic acid) (PLA), poly(glycolic acid) (PGA), poly(lactic-co-glycolic) acid (PLGA), polycaprolactone (PCL), poly(vinyl alcohol) (PVA) and poly(ethylene oxide) (PEO) have been studied as skin scaffolds (Chaudhari et al. 2016; Song et al. 2018). Drugs and therapeutic agents with a controlled release have been incorporated in scaffolds (Mirdailami et al. 2015), and the effects of diverse elements on different stages of wound healing have been studied (Hoppe et al. 2011; Naseri et al. 2017). In addition, neovascularization

✉ Alireza Sadeghi-Avalshahr
sadeghi_av@ymail.com

1 Department of Materials Research, Iranian Academic Center for Education, Culture and Research (ACECR), Khorasan Razavi Branch, Mashhad, Iran

2 Department of Materials Science and Engineering, Faculty of Engineering and Technology, Tarbiat Modares University, Tehran, Iran

3 Department of Biomaterials, College of Biomedical Engineering, AmirKabir University of Technology, Tehran, Iran

4 Stem Cells and Regenerative Medicine Research Group, Iranian Academic Center for Education, Culture and Research (ACECR), Khorasan Razavi Branch, Mashhad, Iran

and angiogenesis have been improved (Frueh et al. 2017), and diverse methods have been developed for the fabrication of scaffolds and mimicking of natural skin structure (Eltom et al. 2019). Nevertheless, there are still ongoing efforts to manufacture high-quality products.

Among different materials used to improve biological properties, peptides and bioactive glasses (BGs) are particularly known for their excellent properties. Peptide sequences generally consist of less than 50 amino acids, which are smaller than proteins, and can be derived from the extracellular matrix (ECM). The small size allows more molecules to be grafted on the surface of biomaterials, which increases the density of active sites exposed to the cells (Maheshwari et al. 2000; Renth and Detamore 2012). Different peptides can be used to promote cell adhesion, proliferation, differentiation, and angiogenesis of biomaterials (Visser et al. 2016). GHK is a tripeptide with the amino acid sequence of glycyl-*l*-histidyl-*l*-lysine (Pickart 2008). High affinity and copper incorporation are significant properties of GHK-Cu (Pickart et al. 2012). Copper acts as a regulator of cell signaling and it affects cell behavior and metabolism. The human peptide GHK-Cu was first discovered by Pickart et al. in human albumin (Pickart 1973). They found that GHK-Cu accelerated wound healing and contraction, and played an anti-inflammatory role (Downey et al. 1985; Pickart 2011). GHK-Cu has also been found in collagen, which is released by collagen degradation in the damaged tissue (Pickart and Margolina 2018). Clinical and histopathological outcomes of GHK-Cu and zinc oxide in open-wound healing have demonstrated that the effect of tripeptide on accelerating wound healing and blood vessel formation is higher than that of zinc oxide (Cangul et al. 2006; Gul et al. 2008). In another study, the incorporation effect of GHK-Cu peptide along with collagen matrix was evaluated on the dermal wound healing. The effect of peptide-incorporated collagen membrane on improving wound healing process was greater than that of collagen matrix. Wounds treated with the former showed higher contraction and cell proliferation compared to the latter (Arul et al. 2005).

BGs are inorganic materials composed of metal oxides such as SiO_2, CaO, P_2O_5, etc. They have demonstrated biocompatibility, bioactivity, biodegradation, antibacterial activity, and angiogenesis which are excellent properties for hard and soft-tissue engineering applications (Fu et al. 2011; Miguez-Pacheco et al. 2015). In recent years, growing attention has been paid to bioactive glasses in soft-tissue engineering (Miguez-Pacheco et al. 2015). As a bioactive material for wound dressing applications, BG with a certain composition and high surface reactivity can bond with soft tissues and accelerates the healing rate (Hench 1996). In particular, studies have shown that the wound healing process can be improved by released ionic products through the control of bacterial microorganisms, blood coagulation, cell proliferation stimulation, angiogenesis, and collagen production (Hench 2006; Zhang et al. 2010). Research has revealed that the stimulating effect of bioactive glass on fibroblast growth factor expression can lead to increased blood vessel formation, differentiation of fibroblasts to myofibroblasts, and improved wound healing (Kargozar et al. 2019). Lin et al. investigated the effect of ointments containing 45S5 and 58S bioactive glasses on cutaneous wound healing in both normal and diabetic rats. They reported that bioactive glasses enhanced wound healing. By analogy, ointment containing 58S BG was faster and more efficient than 45S5 BG in healing wounds (Lin et al. 2012).

Collagen and chitosan, as natural polymers known for their excellent biological properties, have been utilized in many skin tissue engineering studies and products. The poor mechanical properties of these polymers can be compensated with synthetic biodegradable polymers such as PCL. The goal of this research is to explore the effect of adding GHK-Cu and bioactive glass to collagen/chitosan-coated poly(ε-caprolactone) (PCL–Col–Chit) scaffold. We presume that the biological properties of scaffold containing collagen/chitosan can be improved further by GHK-Cu and the bioactive glass.

Materials and methods

Materials

Poly(ε-caprolactone) with average $M_n \sim 80{,}000$, polyvinylpyrrolidone (PVP) with average $M_w \sim 360{,}000$, (3-Aminopropyl)triethoxysilane (APTES, 99%) and glutaraldehyde solution (25%) were purchased from Merck (Germany). Bioactive glass 58S consisting of $58SiO_2 - 33CaO$ to $9P_2O_5$ (wt%) with a particle size of < 150 nm was obtained from Nik Ceram Razi Co. (Iran). The following materials with the highest purity were purchased from commercial distributors: type I collagen sponge from Wuxi Biot Biotechnology Co. Ltd (China); chitosan with $M_w \sim 557{,}000$ from Sigma-Aldrich (China) and peptide GHK-Cu from Pepmic Co. Ltd (China). All other chemicals and reagents were of analytical grade.

Scaffold fabrication

In a recent research, we have fabricated PCL–Col–Chit scaffold by the electrospinning of PCL and then its coating with collagen/chitosan. In short, the PCL solution with a concentration of 20% (w/v) in acetic acid (80% v/v) and PVP solution with a concentration of 25% (w/v) in ethanol were prepared and stirred for 24 h. The co-electrospinning of PCL and PVP solutions was carried out using counter syringes. Flow rates of PCL and PVP solutions were 1 and 0.4 ml/h,

respectively, and other electrospinning parameters were constant for both solutions: Voltage = 25 kV, needle tip to collector distance = 15 cm and needle gauge 22. After 10 h electrospinning, the resultant PCL/PVP scaffold was soaked in distilled water for 48 h to eliminate PVP. This process increased the pore size. The PCL scaffold was aminolyzed in 1,6-hexanediamine/2-propanol solution (10% w/v) at 37 ºC for 45 min by a shaker incubator to introduce NH_2 and OH groups to the surface of PCL fibers. To remove free 1,6-hexanediamine, scaffold samples were rinsed in deionized water (DI water) for 24 h and then dried at room temperature. In the next step, aminolyzed scaffolds were immersed in the glutaraldehyde solution (1% w/v) at room temperature for 3 h, and then rinsed 4–5 times with a large amount of water to remove unreacted glutaraldehyde. Finally, treated scaffolds were soaked in collagen/chitosan solution (acetic acid 0.5 M) at 2–4 ºC for 24 h. The concentration of collagen and chitosan in the solution was 5 and 3 (mg/mL), respectively. The collagen/chitosan-coated scaffolds were immersed in DI water for 30 min, washed twice (to remove free collagen and chitosan) and dried at room temperature.

Bioactive glass coating

Bioactive glass coating of PCL–Col–Chit scaffold and the bonding of BG and collagen were carried out by the silanization process, as described in Ref (Hum and Boccaccini 2018). To do so, first the glass powder was ultrasonicated for 5 min in acetone to remove contaminations and create reactive OH groups. The sonication was carried out under the condition of 100 watts and 28 kHz. Then, the powder was washed three times using filter paper and DI water, and dried at 100 ºC for 1 h. The second step involved immersing glass powder in a solution of APTES (2% v/v) in acetone for 2 h to create siloxane groups on the glass surface, followed by rinsing with DI water twice and drying at 100 ºC for 1 h to replace hydrogen bond with a stronger covalent bond. Finally, three different suspensions of BG with concentrations of 0.01%, 0.1% and 0.5% (w/v) were prepared in DI water and 200 µL/well of each suspension was poured into 12-well plates containing PCL–Col–Chit samples. The coated samples were dried at room temperature. These samples were labeled as BG-0.01, BG0.1, and BG-0.5 proportional to the concentration of the suspensions.

GHK-Cu coating

To coat PCL–Col–Chit scaffolds with GHK-Cu, a solution of peptide in milli-Q water with a concentration of 1 mM was prepared and stirred at 4ºC for 2 h. Then, 200 µL/well of the solution was poured into 12-well plates containing PCL–Col–Chit samples. This sample was labeled as GHK-Cu.

Characterization

FTIR and ATR–FTIR

Fourier transform infrared (FTIR) and Attenuated total reflection–Fourier transform infra-red (ATR–FTIR) spectroscopy was performed at the range of 400–4000 cm^{-1} using a Thermo Nicolet FTIR spectrometer (Avatar 370, USA).

Scanning electron microscopy

The microstructure of scaffolds, before and after coating, was observed using the field emission scanning electron microscope (FESEM) (Tescan-Mira3 LMU, Czech Republic) equipped with an EDS detector.

MTT Assay

The cell viability of samples was assessed using MTT assay [3-(4,5- dimethylthiazol-2-yl)-2,5 diphenyltetrazolium bromide] by counting the number of human dermal fibroblast (HDF) (primary cell line, passage 2, cryopreserved) cultured on samples. The cells were gifted by stem cells and regenerative medicine research group, ACECR. The scaffolds were cut into circular discs with a diameter of 21 mm, disinfected by ethanol 70% and sterilized by UV radiation for 1 h on each side (Dai et al. 2016). The scaffolds were fixed in the autoclaved cell crown-like fixture to avoid cell leakage under scaffolds. In the next step, four samples from each group were placed in a 12-well plate, three samples for cell seeding and one sample without seeding as the negative control. Human dermal fibroblasts with a density of 3×10^4 cm^{-2} were seeded separately on scaffolds and cultured in high glucose Dulbecco's Modified Eagle Medium (DMEM) with 10% FBS and 100 UmL^{-1} penicillin/100 μgmL^{-1} streptomycin. The medium was changed every 3 days. Afterwards, formazan crystals were created by adding 50 µL of 5 mg/mL MTT solution to each well, which were then incubated in 5% CO_2 at 37 °C for 3 h. The MTT reaction medium was removed after incubation and 600 µL/well of dimethyl sulfoxide (DMSO)/isopropanol was added to dissolve crystals. The medium containing cells without scaffold was used as the positive cytotoxicity control. The MTT assay was performed on days 3, 5, and 7. The absorbance was measured at 570 nm by ELISA plate reader (Biotek-Epoch, USA). The cell viability was calculated for each sample and reported after the subtraction of optical density (OD) from the negative control (scaffold without cell seeding).

Cell adhesion

To evaluate cell adhesion, HaCaT cell lines were cultured on samples in duplicate. The sample preparation before cell seeding, which comprised cutting, disinfection and sterilization of scaffolds, resembled the sample preparation for MTT assay. After 3 days of cell culturing, the plates containing scaffolds were washed twice with phosphate-buffered saline (PBS) to remove the unattached cells. The attached cells were fixed in 2.5% glutaraldehyde for 3 h. After removing the fixator, the scaffold was rinsed with PBS and dried in a laminar hood. In the next step, the cell attachment to scaffolds was investigated by FESEM.

Antibacterial assay

The antibacterial activities of PCL, PCL–Col–Chit, GHK-Cu, and BG-0.01 samples were studied with two bacteria species commonly found in burn wounds: Staphylococcus aureus (ATCC 6538, PTCC 1112) as the gram-positive and *Escherichia coli* (ATCC 25922, PTCC 1399) as the gram-negative species. To do so, samples were initially sterilized by UV for 30 min. Then, 500 µL of bacterial suspension (1.5 × 106 CFU/mL) was placed in each sample (with a circular shape and a diameter of 21 mm) and incubated at 37 °C for 1 and 24 h. Afterwards, the samples were placed in some sterile plastic tubes, diluted with PBS and homogenized by centrifuging at 10,000 rpm for 1 min. The solution was cultured on an agar plate and incubated at 37 °C for 48 h. Finally, the antibacterial activity of each sample was measured by counting the number of bacteria colonies and the results were compared to the number of bacteria colonies in the PCL scaffold (control sample) using the following formula:

$$\text{Antibacterial activity } (\%) = \frac{(\text{control} - \text{sample})}{\text{control}} \times 100. \quad (1)$$

Statistical analysis

Data are presented as mean ± standard deviation. Statistical analysis was performed utilizing one-way analysis of variance (ANOVA) using Origin 2018 software. A p value < 0.05 was considered as statistically significant.

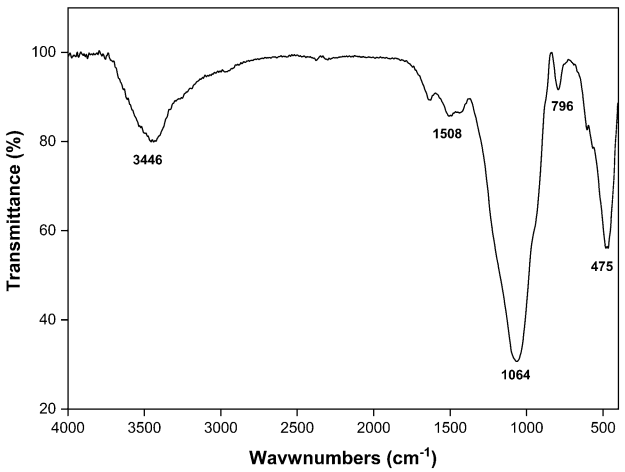

Fig. 1 FTIR spectrum of silanized BG powder

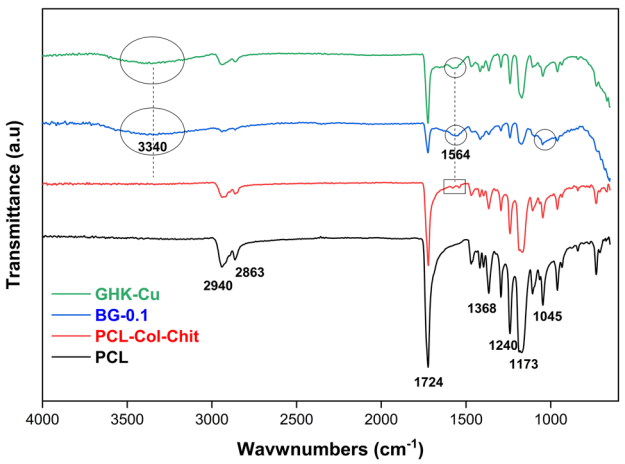

Fig. 2 ATR–FTIR spectra of PCL, PCL–Col–Chit, BG-0.1 and GHK-Cu samples

Results

FTIR and ATR–FTIR

FTIR spectroscopy of silanized BG powder is shown in Fig. 1. The strong and wide peak at 1064 cm^{-1} is attributed to Si–O–Si and P–O stretching vibrations. Additionally, the peaks at 796 cm^{-1} and 475 cm^{-1} are assigned, respectively, to symmetric stretching and bending vibrations of Si–O. The band appeared at around 1508 cm^{-1} is ascribed to N–H bending vibration and the wide peak at 3446 cm^{-1} is related to overlapped stretching mode of O–H and N–H vibrations (Esmaeilzadeh et al. 2017).

Figure 2 shows the ATR–FTIR spectra of PCL, PCL–Col–Chit, BG-0.1 and GHK-Cu samples after

disinfection and sterilization. The main functional groups of PCL at 2800–2950 cm^{-1} (stretching vibration of -CH_2 and -CH_3), 1724 cm^{-1}(carbonyl–C = O), 1368 cm^{-1} (bending vibration of -CH_2) and 1045- 1240 cm^{-1} (C-O) are shown in the figure (Rezaei and Mohammadi 2012). The spectra of PCL and PCL–Col–Chit are very similar except two very weak peaks at 1597 cm^{-1} and 1539 cm^{-1} (aminogroups) which are marked with rectangle. Theses peaks are contributed to collagen and chitosan (Nazemi et al. 2014; Zhao et al. 2015). After modification of PCL–Col–Chit scaffold with BG and GHK-Cu, these peaks are merged into a more intense peak at 1564 cm^{-1}. This peak is attributed to NH_2 which exists in both GHK-Cu and silanized BG. Additionally, a very wide peak is appeared at 3340 cm^{-1} for both samples which is assigned to stretching vibration of OH and NH. Besides, the peak at 1045 cm^{-1} becomes wider and slightly shifts toward higher wave numbers for BG-0.1 sample (Esmaeilzadeh et al. 2017).

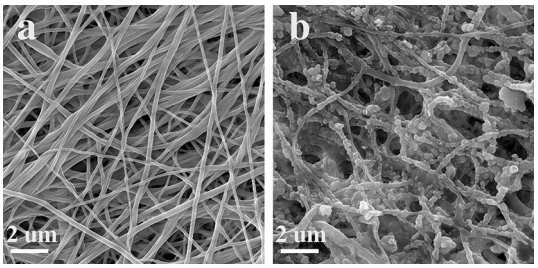

Fig. 3 SEM images of PCL and collagen/chitosan-coated PCL scaffolds

Microstructure and elemental analysis

The microstructure of PCL scaffold and collagen/chitosan-coated PCL scaffold is depicted in Fig. 3a and b, respectively. Collagen and chitosan with a spherical morphology were spread all over the fibrous PCL scaffold. Figure 4a shows back-scattered electron (BSE) image of the sample BG-0.01. The BG glass particles can be distinguished from the collagen/chitosan by their whiter appearance in the BSE mode due to the higher molar mass of their constituents (i.e., Si, Ca and P). (Fig. 4b–h) shows the SEM of agglomerated BG particles and the EDS elemental map scan images of C, O, N, Si, Ca, P. The secondary electron (SE) image and the map scan images of GHK-Cu-coated scaffolds are displayed in Fig. 5a–e.

Cytotoxicityassay

Figure 6 shows the results of MTT assay for the uncoated scaffold (i.e., collagen/chitosan-coated PCL sample) along with GHK-Cu- and 58S BG-coated scaffolds of different concentrations. No cytotoxic effect was observed in no sample after 7 days of cell culturing. After 3 days of cell culturing, GHK-Cu-coated scaffold demonstrated significant improvement in cell viability, but no significant difference was observed on days 5 and 7. There was not any difference between BG-coated samples and uncoated sample after 5 days, but substantial improvement was observed in BG-0.01 and BG-0.1 scaffolds on day 7 in comparison with the uncoated sample.

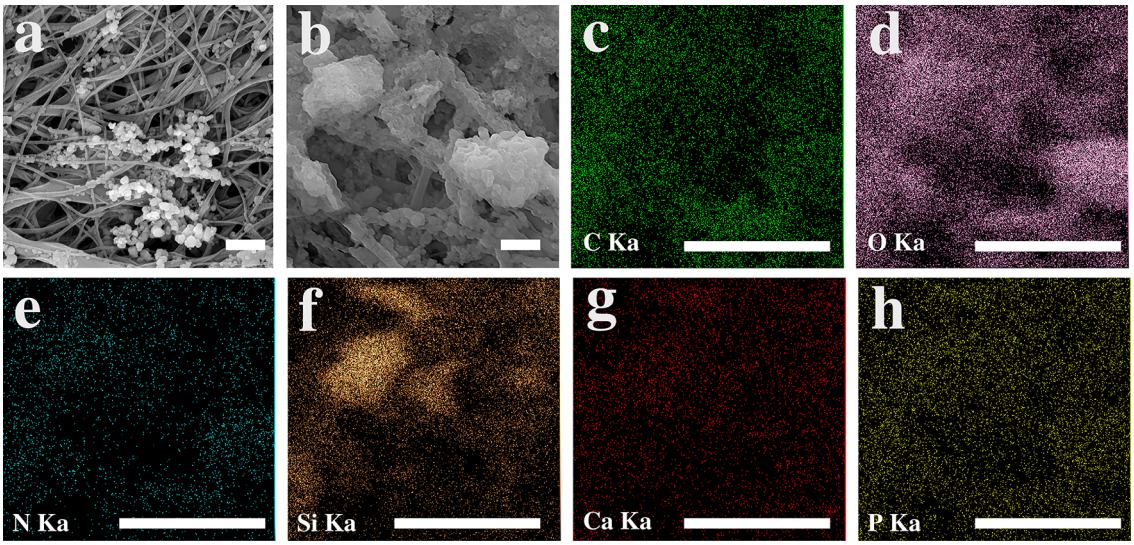

Fig. 4 SEM and EDS elemental mapping of bioactive glass-coated PCL–Col–Chit with a concentration of 0.01 (BG-0.01). **a** Back-scattered electron SEM image, **b** secondary electron SEM image, and (**c**–**h**) EDS map analysis corresponding to image (**b**). The scale bars represent 2 µm

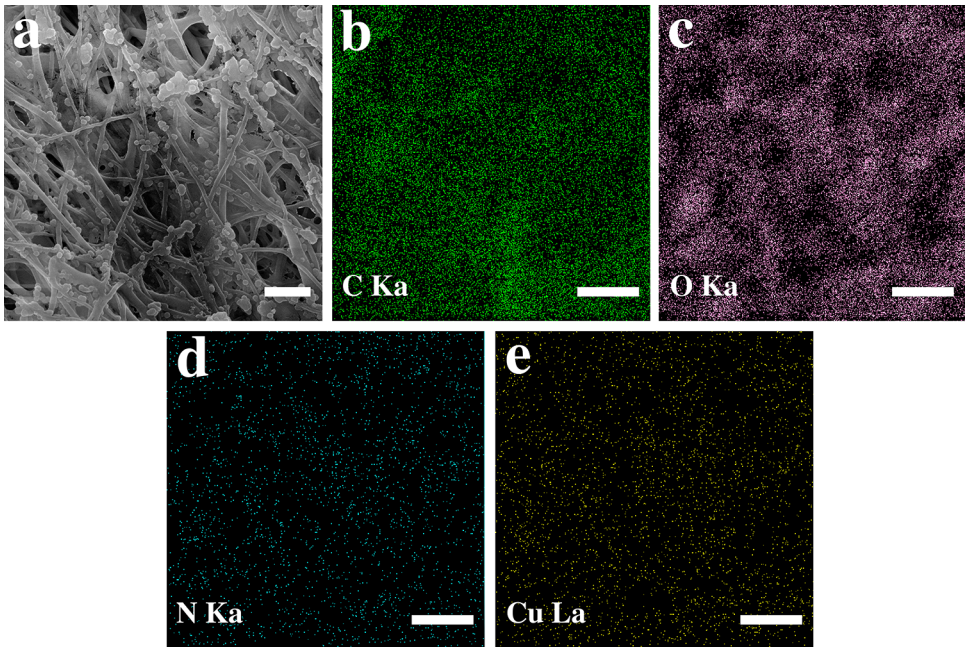

Fig. 5 **a** SEM image and (**b**–**e**) the corresponding elemental distribution map of GHK-Cu-coated scaffold. The scale bars represent 2 µm

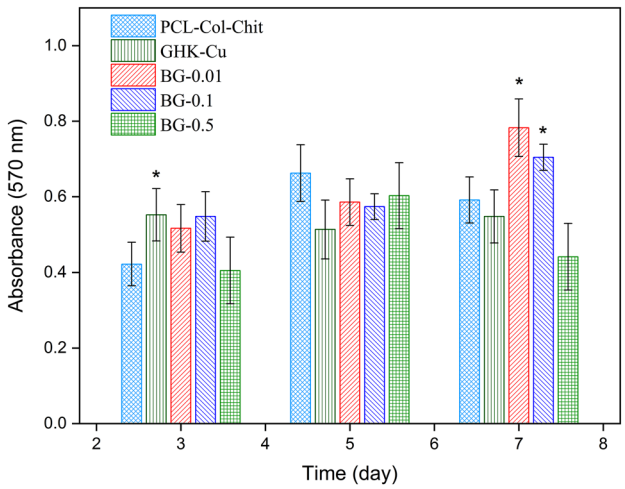

Fig. 6 MTT results of HDF cell seeding on PCL–Col–Chit scaffold (uncoated scaffold), GHK-Cu-coated scaffold and scaffolds coated with diverse concentrations of bioactive glass for 3, 5, and 7 days. Asterisks show the statistically significant changes of coated samples versus uncoated sample at each time point

Cell adhesion

Keratinocyte cell attachment in different samples is shown in Fig. 7. SEM images reveal desirable cellular adhesion in all samples. There was no significant difference in cell attachment between the uncoated and coated scaffolds after 3 days.

Antibacterial test

Figure 8 shows the antibacterial activity for PCL, PCL–Col–Chit, GHK-Cu and BG-0.01 samples. After 1 h, GHK-Cu was the only sample depicting reduced bacteria population, both in Escherichia coli (*E.coli*) and Staphylococcus aureus (*S.aureus*). After 24 h, PCL–Col–Chit, GHK-CU and BG-0.01 scaffolds exhibited antibacterial activities which are more effective at killing gram-negative bacteria. However, GHK-Cu showed superior anti-bacterial characteristics at this time point.

Discussion

The appearance of peak at 1508 cm^{-1} in Fig. 1 may indicate the emerging of reactive aminogroups on the BG surface. These functional groups play role as a coupling agent between BG and collagen (Hum and Boccaccini 2018). Compared to the ATR–FTIR pattern of PCL–Col–Chit, the intense NH_2 band at 1564 cm^{-1} and the emerging of new band of O–H and N–H vibrations centered at 3340 cm^{-1} prove the successful surface modification of PCL–Col–Chit scaffold with GHK-Cu and BG (Fig. 2).

The microstructure and surface features of a scaffold can substantially influence its biological properties. These characteristics include fiber diameter, pore size distribution, total porosity, surface roughness and morphology of coated materials. In this study, the primary scaffold consists of non-woven PCL fibers with considerable surface roughness caused by collagen/chitosan coating. After coating with the peptide, no tangible changes were observed in

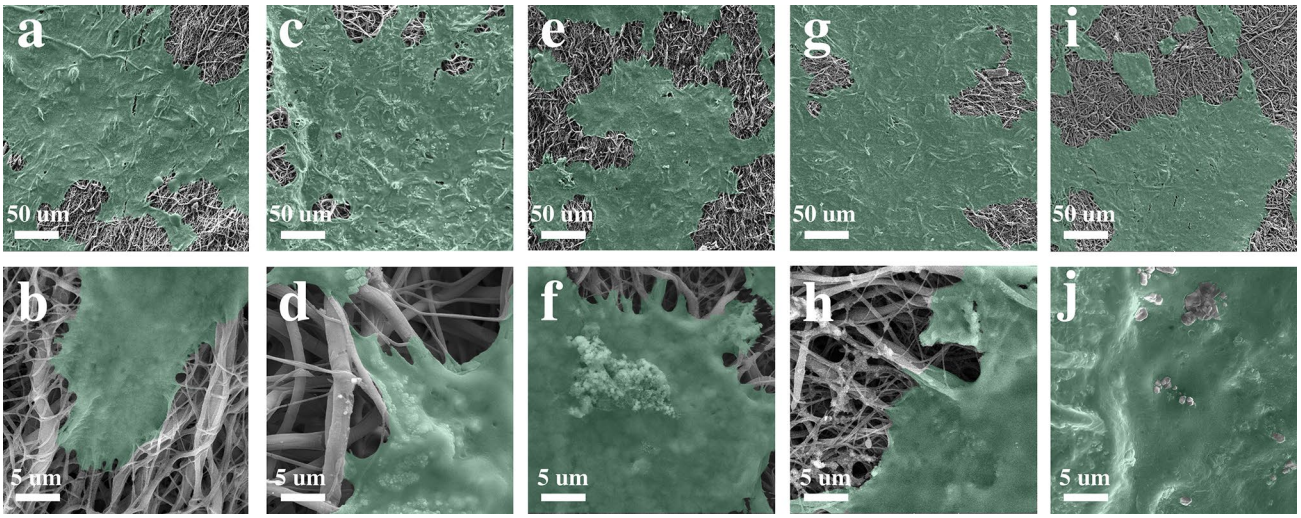

Fig. 7 SEM images of cell attachment for (**a**, **b**) uncoated scaffold; (**c**, **d**) GHK-Cu coated; (**e**, **f**) BG-0.01, (**g**, **h**) BG-0.1, and (**i**, **j**) BG-0.5 scaffolds under 500 × and 5000 × magnifications

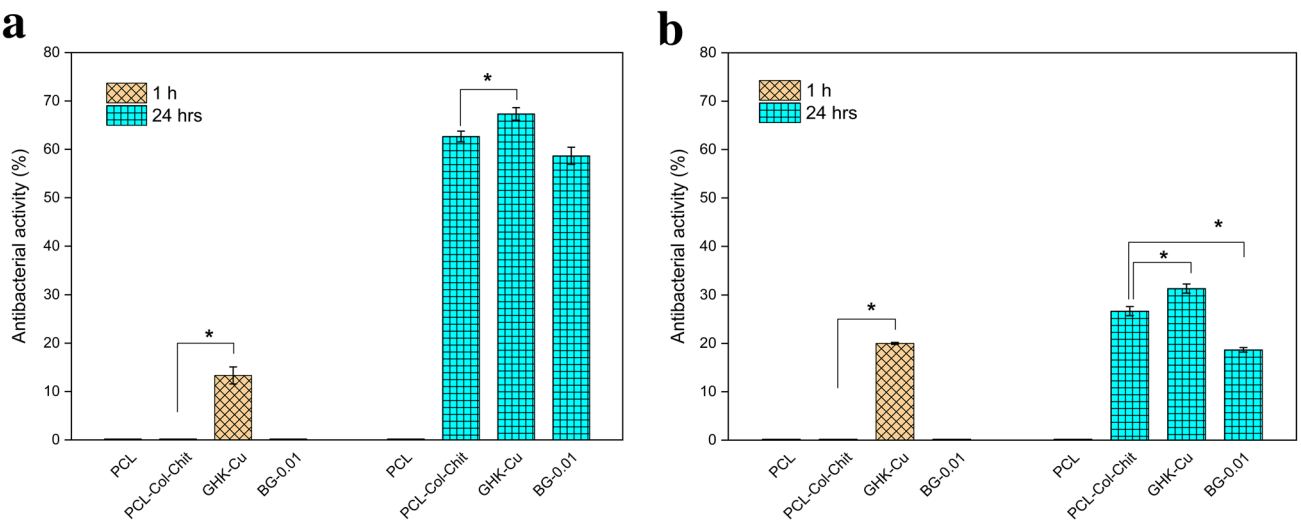

Fig. 8 Antibacterial activity (%) of PCL, PCL–Col–Chit, GHK-Cu and BG-0.01 against **a** *E.coli* and **b** *S. aureus* after 1 and 24 h. Asterisks show the statistically significant changes of GHK-Cu and BG-0.01 compared to PCL–Col–Chit at each time point

the microstructure of GHK-Cu (Fig. 5a); while in the BG-coated samples, both nano-sized and agglomerated particles were observed (Fig. 4a, b). EDS and elemental mapping confirmed the presence of GHK-Cu and BG in the coated scaffolds.

To study cell adhesion properties of different scaffolds, keratinocyte cell attachment was investigated after 3 days of seeding (Fig. 7). All scaffolds revealed cell adhesion. However, the cell adhesion for PCL–Col–Chit, GHK-Cu and BG-coated samples was more desirable. Although PCL is a hydrophobic polymer, coating PCL fibers with collagen and chitosan makes the scaffold hydrophilic. Hydrophilicity boosts cell-scaffold interaction. Also, collagen is composed of three polypeptide subunits, which can act as an integrin receptor of cells (Davidenko et al. 2018). With the exception of compositional properties, microstructural parameters of a scaffold such as pore size, fiber diameter, and surface roughness are determinants of cell-to-scaffold attachment. For PCL–Col–Chit scaffold, the pore diameter is in the range of 7–140 µm and the average fiber diameter is 339 ± 122 nm which are suitable for cell attachment (Kumbar et al. 2008). Moreover, the rough surface of the scaffold induced by collagen/chitosan coating can promote cell adhesion (Zamani et al. 2013; Levengood and Zhang 2014). As shown in Fig. 7a and b, these parameters provide a favorable ground for cell attachment to PCL–Col–Chit scaffold, and

the addition of GHK-Cu and bioactive glass has not significantly improved cell attachment.

Collagen and chitosan are natural polymers that stimulate cell proliferation (Ho et al. 2014; Sadeghi et al. 2016; Dong and Lv 2016). In the uncoated scaffold, fibroblast cell viability rose on days 5 and 7 compared to day 3. This can be attributed to the ability of collagen and chitosan to stimulate proliferation. However, coating the scaffold with GHK-Cu or BG improved cell viability. After 3 days of cell culturing, the viability of fibroblast cells was enhanced significantly in the GHK-Cu sample compared to the uncoated scaffold. This finding is consistent with those reported by Arul et al. 2005, according to which, incorporating the GHK in the collagen enhanced fibroblast cell proliferation. The effect of GHK-Cu on the stimulation of keratinocyte cell proliferation has also been reported (Kang et al. 2009). Also, bioactive glass-coated scaffolds with concentrations of 0.01 and 0.1 exhibited cell proliferation improvement on day 7 compared to the PCL–Col–Chit sample. This can be attributed to ionic dissolution products of the bioactive glass, which can stimulate reactions with cells and enhance proliferation (Mortazavi et al. 2010). Valerio et al. reported augmented osteoblast cell proliferation due to the effects of bioactive glass dissolution and the release of ionic products (Valerio et al. 2004).

Besides biocompatibility and bioactivity, the antibacterial activity of a scaffold is essential for wound healing. Antibacterial properties of PCL–Col–Chit, GHK-Cu and BG-0.01 samples are presented in Fig. 8. Among bioactive glass-coated scaffolds, BG-0.01 sample was selected for the antibacterial test since this sample exhibited superior cell proliferation in the MTT assay. Also, the antibacterial activity of PCL scaffold was evaluated as the control sample in this test. The PCL–Col–Chit scaffold demonstrated favorable bacterial killing properties in comparison with the PCL scaffold after 24 h, especially for gram-negative bacteria. The antibacterial characteristic of this sample could be attributed to the chitosan, which is known for its antibacterial activity. Three possible mechanisms have been proposed for antibacterial properties of chitosan. First, chitosan surface is positively charged, which can interact with negative charges of bacterial cell membrane. This interaction results in the leakage of intracellular electrolytes and the growth inhibition of microorganism due to the alteration of cell wall permeability. Second, chitosan penetrates through bacterial cell wall and binds with bacterial DNA. Third, metals are chelated and the flow of nutrients is obstructed (Kim 2018).

One interesting observation was that the antibacterial characteristic of PCL–Col–Chit scaffold was improved by GHK-Cu coating. After 1 h, GHK-Cu-coated sample, unlike the uncoated sample, revealed antibacterial activity. Also after 24 h, the antibacterial activity of the former was greater than the latter. The excellent antibacterial properties of GHK-Cu could be attributed to Cu^{2+}. Copper has been introduced as the first solid antibacterial material by the U.S. Environmental Protection Agency (Grass et al. 2011). Cu^{+2} could be released form GHK-Cu due to the unstable nature of this peptide in biological fluids (Sun et al. 2019).

The BG-0.01 exhibited desirable antibacterial activity against both *E.coli* and *S.aureus* after 24 h, but the scale of its activity was less than the uncoated scaffold. Two mechanisms have been proposed for antibacterial properties of bioactive glasses: (1) the dissolution of BG and the release of ions increase pH locally, and create a hostile environment for bacteria, (2) the release of ions leads to an elevated solute concentration and, therefore, higher osmotic pressure (Drago et al. 2018). Hence, the degradation rate is a determinant of antibacterial properties in BGs. This characteristic depends on the glass composition, particle size and environmental pH. In the present study, the pH of BG-0.01 scaffold remained unchanged after 24 h. It can be concluded that higher amounts of BG or longer time periods are required to improve the antibacterial activity of the BG-coated sample.

Conclusion

In this study, biological properties of PCL–Col–Chit fibrous scaffolds (uncoated scaffold), GHK-Cu and bioactive glass-coated scaffolds were studied under in vitro condition. All samples exhibited favorable cell attachment. The cell viability of GHK-Cu sample improved compared to the uncoated scaffold after 3 days of cell culturing. BG-0.01 and BG-0.1 samples indicated substantial cell viability enhancement compared to the uncoated sample on day 7. PCL–Col–Chit, GHK-CU and BG-0.01 exhibited antibacterial activity against *E.coli* and *S.aureus* after 24 h, though the activity of GHK-Cu-coated sample was greater than other samples. GHK-Cu also revealed considerable antibacterial activity after 1 h. Overall, the experiments suggested that GHK-Cu and bioactive glass coating could improve biological properties of the collagen/chitosan-coated PCL scaffold.

Acknowledgements This study was financially supported by Academic Center for Education, Culture and Research (ACECR) Grant Number: 5005-20.

Author contributions All authors contributed to the conceptualization and design. Material preparation, experiments and data analysis were performed by AMM, ARS, and SN. The first draft of the manuscript was written by AMM and all authors read and approved the final manuscript.

Compliance with ethical standards

Conflict of interest The authors declare that there is no conflict of interests.

Ethical approval This article does not contain any studies with human participants or animals performed by any of the authors.

References:s

Arul V, Gopinath D, Gomathi K, Jayakumar R (2005) Biotinylated GHK peptide incorporated collagenous matrix: a novel biomaterial for dermal wound healing in rats. J Biomed Mater Res Part B Appl Biomater 73B:383–391. https://doi.org/10.1002/jbm.b.30246

Boyce ST, Lalley AL (2018) Tissue engineering of skin and regenerative medicine for wound care. Burn Trauma 6:4. https://doi.org/10.1186/s41038-017-0103-y

Cangul IT, Gul NY, Topal A, Yilmaz R (2006) Evaluation of the effects of topical tripeptide-copper complex and zinc oxide on open-wound healing in rabbits. Vet Dermatol 17:417–423. https://doi.org/10.1111/j.1365-3164.2006.00551.x

Chaudhari A, Vig K, Baganizi D et al (2016) Future prospects for scaffolding methods and biomaterials in skin tissue engineering: a review. Int J Mol Sci 17:1974. https://doi.org/10.3390/ijms17121974

Dai Z, Ronholm J, Tian Y et al (2016) Sterilization techniques for biodegradable scaffolds in tissue engineering applications. J Tissue Eng 7:204173141664881. https://doi.org/10.1177/2041731416648810

Davidenko N, Hamaia S, Bax DV et al (2018) Selecting the correct cellular model for assessing of the biological response of collagen-based biomaterials. Acta Biomater 65:88–101. https://doi.org/10.1016/j.actbio.2017.10.035

Dong C, Lv Y (2016) Application of collagen scaffold in tissue engineering: recent advances and new perspectives. Polymers (Basel) 8:42. https://doi.org/10.3390/polym8020042

Downey D, Larrabee WF, Voci V, Pickart L (1985) Acceleration of wound healing using glycyl-histidyl-lysine copper (II). Surg Forum 25:573–575

Drago L, Toscano M, Bottagisio M (2018) Recent evidence on bioactive glass antimicrobial and antibiofilm activity: a mini-review. Materials 11(3):326. https://doi.org/10.3390/ma11020326

Eltom A, Zhong G, Muhammad A (2019) Scaffold techniques and designs in tissue engineering functions and purposes: a review. Adv Mater Sci Eng 2019:1–13. https://doi.org/10.1155/2019/3429527

Esmaeilzadeh J, Hesaraki S, Hadavi SM-M et al (2017) Poly (d/l) lactide/polycaprolactone/bioactive glasss nanocomposites materials for anterior cruciate ligament reconstruction screws: the effect of glass surface functionalization on mechanical properties and cell behaviors. Mater Sci Eng C 77:978–989. https://doi.org/10.1016/j.msec.2017.03.134

Frueh FS, Menger MD, Lindenblatt N et al (2017) Current and emerging vascularization strategies in skin tissue engineering. Crit Rev Biotechnol 37:613–625. https://doi.org/10.1080/07388551.2016.1209157

Fu Q, Saiz E, Rahaman MN, Tomsia AP (2011) Bioactive glass scaffolds for bone tissue engineering: State of the art and future perspectives. Mater Sci Eng C 31:1245–1256. https://doi.org/10.1016/j.msec.2011.04.022

Grass G, Rensing C, Solioz M (2011) Metallic copper as an antimicrobial surface. Appl Environ Microbiol 77:1541–1547. https://doi.org/10.1128/AEM.02766-10

Gul NY, Topal A, Cangul IT, Yanik K (2008) The effects of topical tripeptide copper complex and helium-neon laser on wound healing in rabbits. Vet Dermatol 19:7–14. https://doi.org/10.1111/j.1365-3164.2007.00647.x

Hench LLWJ (1996) Biological applications of bioactive glasses. Life Chem Rep 13:187–241

Hench LL (2006) The story of bioglass®. J Mater Sci Mater Med 17:967–978. https://doi.org/10.1007/s10856-006-0432-z

Ho MH, Liao MH, Lin YL et al (2014) Improving effects of chitosan nanofiber scaffolds on osteoblast proliferation and maturation. Int J Nanomed 9:4293–4304. https://doi.org/10.2147/IJN.S68012

Hoppe A, Güldal NS, Boccaccini AR (2011) A review of the biological response to ionic dissolution products from bioactive glasses and glass-ceramics. Biomaterials 32:2757–2774. https://doi.org/10.1016/j.biomaterials.2011.01.004

Hum J, Boccaccini AR (2018) Collagen as coating material for 45S5 bioactive glass-based scaffolds for bone tissue engineering. Int J Mol Sci. https://doi.org/10.3390/ijms19061807

Kang YA, Choi HR, Na JI et al (2009) Copper-GHK increases integrin expression and p63 positivity by keratinocytes. Arch Dermatol Res 301:301–306. https://doi.org/10.1007/s00403-009-0942-x

Kargozar S, Mozafari M, Hamzehlou S, Baino F (2019) Using bioactive glasses in the management of burns. Front Bioeng Biotechnol. https://doi.org/10.3389/fbioe.2019.00062

Kim S (2018) Competitive biological activities of chitosan and its derivatives: antimicrobial, antioxidant, anticancer, and anti-inflammatory activities. Int J Polym Sci. https://doi.org/10.1155/2018/1708172

Kumbar SG, Nukavarapu SP, James R et al (2008) Electrospun poly(lactic acid-co-glycolic acid) scaffolds for skin tissue engineering. Biomaterials 29:4100–4107. https://doi.org/10.1016/j.biomaterials.2008.06.028

Levengood SKL, Zhang M (2014) Chitosan-based scaffolds for bone tissue engineering. J Mater Chem B 2:3161. https://doi.org/10.1039/c4tb00027g

Lin C, Mao C, Zhang J et al (2012) Healing effect of bioactive glass ointment on full-thickness skin wounds. Biomed Mater 7:045017. https://doi.org/10.1088/1748-6041/7/4/045017

Maheshwari G, Brown G, Lauffenburger DA et al (2000) Cell adhesion and motility depend on nanoscale RGD clustering. J Cell Sci 113:1677–1686

Miguez-Pacheco V, Hench LL, Boccaccini AR (2015) Bioactive glasses beyond bone and teeth: emerging applications in contact with soft tissues. Acta Biomater 13:1–15. https://doi.org/10.1016/j.actbio.2014.11.004

Mirdailami O, Soleimani M, Dinarvand R et al (2015) Controlled release of rhEGF and rhbFGF from electrospun scaffolds for skin regeneration. J Biomed Mater Res Part A 103:3374–3385. https://doi.org/10.1002/jbm.a.35479

Mortazavi V, Mehdikhani Nahrkhalaji M, Fathi MH et al (2010) Antibacterial effects of sol-gel-derived bioactive glass nanoparticle on aerobic bacteria. J Biomed Mater Res Part A 94:160–168. https://doi.org/10.1002/jbm.a.32678

Naseri S, Lepry WC, Nazhat SN (2017) Bioactive glasses in wound healing: hope or hype? J Mater Chem B 5:6167–6174. https://doi.org/10.1039/C7TB01221G

Nazemi K, Moztarzadeh F, Jalali N et al (2014) Synthesis and characterization of poly(lactic-co-glycolic) acid nanoparticles-loaded chitosan/bioactive glass scaffolds as a localized delivery system in the bone defects. Biomed Res Int 2014:1–9. https://doi.org/10.1155/2014/898930

Pickart L (1973) A tripeptide from human serum which enhances the growth of neoplastic hepatocytes and the survival of normal hepatocytes. Biochemistry. University of California, San Francisco

Pickart L (2008) The human tri-peptide GHK and tissue remodeling. J Biomater Sci Polym Ed 19:969–988. https://doi.org/10.1163/156856208784909435

Pickart L (2011) Iamin: a human growth factor with multiple wound-healing properties. Biol Copp Complexes. https://doi.org/10.1007/978-1-4612-4584-1_21

Pickart L, Margolina A (2018) Regenerative and protective actions of the ghk-cu peptide in the light of the new gene data. Int J Mol Sci. https://doi.org/10.3390/ijms19071987

Pickart L, Vasquez-Soltero JM, Margolina A (2012) The human tripeptide GHK-Cu in prevention of oxidative stress and degenerative conditions of aging: implications for cognitive health. Oxid Med Cell Longev 2012:1–8. https://doi.org/10.1155/2012/324832

Renth AN, Detamore MS (2012) Leveraging "raw materials" as building blocks and bioactive signals in regenerative medicine. Tissue Eng Part B Rev 18:341–362. https://doi.org/10.1089/ten.teb.2012.0080

Rezaei A, Mohammadi MR (2012) Development of hydroxyapatite nanorods-polycaprolactone composites and scaffolds derived from a novel in-situ sol-gel process. Tissue Eng Regen Med 9:295–303. https://doi.org/10.1007/s13770-012-0002-z

Sadeghi AR, Nokhasteh S, Molavi AM et al (2016) Surface modification of electrospun PLGA scaffold with collagen for bioengineered skin substitutes. Mater Sci Eng C 66:130–137. https://doi.org/10.1016/j.msec.2016.04.073

Song R, Murphy M, Li C et al (2018) Current development of biodegradable polymeric materials for biomedical applications. Drug Des Dev Ther 12:3117–3145. https://doi.org/10.2147/DDDT.S165440

Sun L, Li A, Hu Y et al (2019) Self-assembled fluorescent and antibacterial GHK-Cu nanoparticles for wound healing applications. Part Part Syst Charact. https://doi.org/10.1002/ppsc.201800420

Valerio P, Pereira MM, Goes AM, Leite MF (2004) The effect of ionic products from bioactive glass dissolution on osteoblast proliferation and collagen production. Biomaterials 25:2941–2948. https://doi.org/10.1016/j.biomaterials.2003.09.086

Vig K, Chaudhari A, Tripathi S et al (2017) Advances in skin regeneration using tissue engineering. Int J Mol Sci 18:789. https://doi.org/10.3390/ijms18040789

Visser R, Rico-Llanos GA, Pulkkinen H, Becerra J (2016) Peptides for bone tissue engineering. J Control Release 244:122–135. https://doi.org/10.1016/j.jconrel.2016.10.024

Zamani F, Amani-Tehran M, Latifi M, Shokrgozar MA (2013) The influence of surface nanoroughness of electrospun PLGA nanofibrous scaffold on nerve cell adhesion and proliferation. J Mater Sci Mater Med 24:1551–1560. https://doi.org/10.1007/s10856-013-4905-6

Zhang D, Leppäranta O, Munukka E et al (2010) Antibacterial effects and dissolution behavior of six bioactive glasses. J Biomed Mater Res Part A 93:475–483. https://doi.org/10.1002/jbm.a.32564

Zhao P, Han F, Zhang P et al (2015) Hydroxyapatite-doped polycaprolactone nanofiber membrane improves tendon and ndash;bone interface healing for anterior cruciate ligament reconstruction. Int J Nanomed. https://doi.org/10.2147/IJN.S92099